

RESEARCH

Open Access



# Increasing apoptosis induction and minimizing side effects of biosynthesized silver nanoparticles by utilizing halloysite nanotubes containing folic acid

Mostafa Heidari Majd<sup>1</sup>, Kimia Behrouz Moghadam<sup>2</sup> and Hong Wang<sup>3\*</sup> 

\*Correspondence:  
Hongwang1985@hotmail.com

<sup>1</sup> Department of Medicinal Chemistry, Faculty of Pharmacy, Zabol University of Medical Sciences, Zabol, Iran

<sup>2</sup> Student Research Committee, Zabol University of Medical Sciences, Zabol, Iran

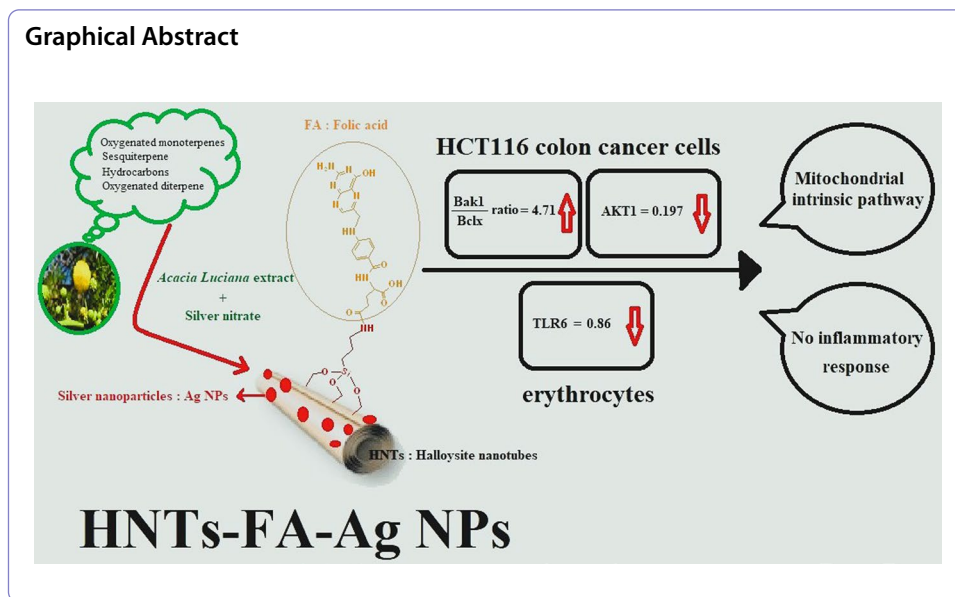
<sup>3</sup> Department of Gastroenterological Surgery, Shandong Provincial Third Hospital, Jinan 250031, China

## Abstract

Since silver nanoparticles (Ag NPs) may not perform well due to low solubility and passive entry, two types of drug delivery systems based on halloysite nanotubes (HNTs) were synthesized. These systems aim to increase the performance and solubility of Ag NPs, as well as enhance their delivery to HCT116 colon cancer cells using folic acid (FA). Ag NPs were successfully anchored onto the surface of HNTs using *Acacia luciana* flower extract, marking a novel approach that led to the synthesis of HNTs-Ag NPs and HNTs-FA-Ag NPs. The cytotoxicity assay showed that even at the lowest concentration, HNTs-FA-Ag NPs can reduce cell viability to below 30% after 48 and 72 h of treatment. They are even more effective than cisplatin. The effectiveness of the synthesized HNTs in inhibiting the growth of cancer cells was further confirmed by staining the protein content of the cells with sulforhodamine B. Real-time PCR results indicated that the presence of FA in the structure of HNTs-FA-Ag NPs activates the mitochondrial intrinsic pathway in HCT116 cells, leading to a 4.71-fold increase in the expression ratio of Bak1/Bclx compared to the control. Furthermore, the reduction in the expression of AKT1, a protein responsible for cell survival and treatment resistance, by HNTs-FA-Ag NPs can be attributed to the presence of FA. This enhances the ability of Ag NPs to inhibit metastases of HCT116 cells. Finally, both modified HNTs demonstrated a protective impact on erythrocytes and reduced oxidative stress. Specifically, HNTs-FA-Ag NPs did not induce any inflammatory response in erythrocytes and did not increase TLR6 gene expression. Therefore, it is expected that HNTs-FA-Ag NPs possess therapeutic capabilities with fewer side effects.

**Keywords:** Colon cancer, AKT1, Bak1/Bclx ratio, TLR6, Ag NPs, Oxidative stress, *Acacia luciana*





## Introduction

Halloysite nanotubes (HNT) are aluminosilicate clay minerals that have the potential to be used as a green and environmentally friendly carrier for loading active and functional agents in the chemical and medical industries (Li et al. 2021). The unique properties of HNTs are due to their hollow tubular structure, with Al–OH groups folded inside and Si–O–Si groups on the external surface, forming a lumen of 10–40 nm, an outward diameter of 50–70 nm, and a length of approximately 100–1000 nm (Ganguly et al. 2018). It has been proven that HNTs have a positively charged inner surface and a negatively charged outer surface at neutral pH (Cheng et al. 2020; Luo et al. 2020). This large internal, external, or even interlayer area allows compounds of appropriate size (on the nanometer scale) to be absorbed. Depending on the molecular mass, interactions with HNTs, and solubility, these compounds can spread well in the physiological environment, with their release ranging from a few hours to two weeks (Karewicz et al. 2021; Wu et al. 2018).

Moreover, halloysite nanotubes (HNTs) are unique in that they allow for the simultaneous immobilization or separate modification by two or more different functional groups. This is possible due to the distinct chemical structures of their internal and external surfaces (Ghalei et al. 2021). One such ligand that can be attached to HNTs to enhance their ability to target tumors and actively identify them, while also reducing side effects, is folic acid (FA) (Wu et al. 2018). Folate receptors (FRs) are typically not expressed in normal cells, but are overexpressed in various human tumors such as ovarian, uterine, endometrial, kidney, brain, cervix, rhinitis, breast, and colon tumors. Therefore, FA is widely used as a crucial ligand for the specific labeling of cancer cells (Leamon and Reddy 2004). On the other hand, there is evidence supporting the chemo-preventive role of FA in colorectal cancer. A deficiency of FA in the diet may alter the expression of genes involved in cell cycle control, cell death, and DNA repair, ultimately increasing the risk of colon cancer (Zsigrai et al. 2022). Additionally, a study by Attias et al. revealed

that FA can suppress IGF-IR gene expression in a p53-dependent manner. These findings suggest that FA can exert its pro-apoptotic effect by enhancing the expression and/or activation of p53 (Attias et al. 2006).

The tumor suppressor p53 gene plays an important role in mitochondria in the induction of apoptosis and cell cycle regulation (Deng et al. 2012). Many studies have confirmed that the reduction of mitochondrial membrane potential initiates the intrinsic cell death pathway and can stimulate the mitochondrial apoptosis pathway by activating Bak and inactivating Bcl-2 (Leibowitz and Yu 2010). Subsequently, cytochrome c passes through the mitochondrial intermembrane space and enters the cytosol to activate effector caspase-3 (Urbani et al. 2020). Caspases can also be activated through the extrinsic pathway of apoptosis depending on TNF or Fas (Muntané 2011). On the other hand, Akt, a physiological substrate of caspase-3, is a major inhibitor of cell apoptosis. One study predicted that the cleavage and inactivation of Akt depends on the activity of caspase-3, suggesting that caspase-3 attenuation may inhibit apoptosis and increase cancer tumor survival (Jahani-Asl et al. 2007). Therefore, we aim to investigate the effect of halloysite nanotubes (HNTs) modified with folic acid (FA) and decorated with green-synthesized silver nanoparticles (Ag NPs) on the expression of genes involved in the intrinsic and extrinsic pathways of apoptosis, as well as genes involved in inhibiting apoptosis and treatment resistance in a human colorectal cancer cell line (HCT116). Additionally, by comparing the effects of HNTs with and without a targeting agent, we hope to determine the role of FA in gene expression. Furthermore, we will explore the potential oxidative stress and inflammation caused by modified HNTs on erythrocytes using lipid peroxidation assays and real-time PCR.

As an effective agent, Ag NPs were synthesized using green methods with *Acacia luciana* flower extract directly on the surface of modified HNTs. Previous work has shown the cytotoxic and apoptotic effects of pure biosynthesized Ag NPs on cancer cell lines (Sargazi et al. 2020). In this study, we aim to investigate the impact of HNTs as carriers and targeting agents on the ability to induce apoptosis and reduce the side effects of Ag NPs.

## Experimental procedures

### Materials

All materials and solvents required for the synthesis of HNTs-Ag NPs and HNTs-FA-Ag NPs were purchased from Sigma-Aldrich Company (Taufkirchen, Germany) and Merck (Darmstadt, Germany). HCT116 cell lines were obtained from the Pasteur Institute (Tehran, Iran). The cDNA synthesis kit was acquired from Pars Tous Biotechnology (Mashhad, Iran) and the RNA Isolation kit was obtained from Roche (Rotkreuz, Switzerland). MTT (3-(4,5-dimethylthiazol-2yl)-2,5 diphenyl tetrazolium bromide), trichloroacetic acid (TCA), and Tris base were received from Merck (Darmstadt, Germany). Sulforhodamine B (SRB) was obtained from Sigma-Aldrich (Taufkirchen, Germany). Fetal bovine serum (FBS) was acquired from PAN Biotech (Aidenbach, Germany). Penicillin/streptomycin and trypsin were bought from Gibco (Carlsbad, USA). RPMI was provided by VIVA CELL (Isfahan, Iran).

### Modification of halloysite nanotubes with folic acid (HNTs-FA)

First, in order to reduce the length, 150 mg of HNTs were added to 10 mL of PBS and subjected to ultrasonic waves at 100% power for half an hour using a probe sonicator (Luo et al. 2020). Afterwards, the mixture was centrifuged at 500 rpm for 10 min, and the obtained sediment was dried at 60 °C for 2 days. After that, 100 mg (0.34 mmol) of shortened HNTs was added to 8 mL of toluene in a flat bottom flask, then 0.079 mL of APTES (0.34 mmol) and 5 µL of TEA were added to the reaction mixture, and refluxed for 24 h using a heater stirrer at 80 °C and 500 rpm. After the completion of the reaction, the obtained HNTs-APTES were washed with ethanol (four times), collected with the help of a centrifuge (950 rpm, 6 min), and dried for 24 h at 60 °C. The grafting yield for this step was calculated to be 92.5%.

For activating the carboxyl group of FA, 139.53 mg (0.32 mmol) of FA, 40.2 mg (0.35 mmol) of NHS, 71.74 mg (0.35 mmol) of DCC and 500 µL of TEA were dissolved in 10 mL of DMSO (Majd 2022). Then, the reaction was continued on a magnetic stirrer (500 rpm) for 24 h under the argon blanket at RT. Afterward, all obtained HNTs-APTES were added to the reaction solution and stirred for another 24 h under the same conditions. After the completion of the reaction, unreacted NHS and DCC were separated using hexane, and the obtained HNTs-FA was washed with acetone (three times) and participated with the help of a centrifuge (950 rpm, 6 min) and dried using a rotary vacuum dryer. The conjugation yield for this step was calculated to be 72%.

### Collection and extraction from *Acacia luciana* flowers

*Acacia luciana* flowers were collected in April from the outskirts of Iranshahr city (southeast of Iran) in Sistan and Baluchistan province (Yan and Majd 2021). Afterwards, 10 g of clean and dry *Acacia luciana* flower powder was transferred in a large Erlenmeyer flask containing 100 mL of 60% ethanol and placed on an orbital shaker for 3 days at 250 rpm. The obtained extract was centrifuged at 1000 rpm for 10 min and the precipitate was discarded. Finally, the supernatant was dehumidified utilizing a freeze dryer at – 60 °C for 2 days.

### Synthesis of HNTs-Ag NPs

We used the previous method in our previous work to decorate HNTs and HNTs-FA with Ag NPs (Zhang and Heidari 2023). For this purpose, 100 mg of HNTs and HNTs-FA were dissolved separately in 25 mL sterile water and 50 mg of silver nitrate was added to them and mixed well at 50 °C. Then 50 mg of *Acacia luciana* extract which is in powder form was added to every reaction mixture and stirred until its color turned dark, then the final products were collected by centrifuge. Hydrochloric acid (0.01 M) was used for the titration of supernatant to obtain the amount of Ag NPs loaded on the surface of both HNTs-Ag NPs and HNTs-FA-Ag NPs.

### Optimization steps in green synthesis

Various optimization steps were carried out in the green synthesis process. This included determining the ideal time for harvesting flowers, the appropriate quantity of dry flowers

for extraction, the correct volume ratio of solvent, and the duration of the extraction process needed to extract *Acacia luciana* flower extract. Furthermore, the amount of silver nitrate, *Acacia luciana* extract, and the reaction temperature were all optimized for the synthesis of HNTs-Ag NPs.

#### **Characterization of modified HNTs**

The initial identification of modified HNTs was done by Fourier transform infrared (FT-IR) spectroscopy. For this purpose, each sample was mixed with KBr moisture-free and turned into a homogenous powder then turned into a thin disk with vacuum at high pressure. The FT-IR device (Shimadzu IR PRESTIGE 21 spectrophotometer, Tokyo, Japan) can scan the region of 4000 to 400  $\text{cm}^{-1}$  and detect the bending and stretching vibrations of molecules.

In order to compare the surface charge of HNTs-Ag NPs and HNTs-FA-Ag NPs together, 2 mg of each modified HNTs was diluted in 10 mL of distilled water. Then, a particle size analyzer (Malvern Zetasizer\_nanoZS, England) device was used to determine their zeta potential in suspension at the range of 200 to  $-200$  mV.

The field emission scanning electron microscope (FESEM) is equipped with a comprehensive range of detectors, which is suitable for routine morphological characterization and size determination of the synthesized nanotubes. For this purpose, HNTs-Ag NPs and HNTs-FA-Ag NPs were placed inside the TESCAN MIRA3 XMU FESEM device after taking the gold coating and photographed with 75 kx magnification. It is also possible to perform elemental analysis of HNTs-Ag NPs and HNTs-FA-Ag NPs using the energy dispersive X-ray (EDX) method. FESEM devices are typically equipped with EDX and can be used for elemental analysis. This analysis helps determine the accuracy of synthesis by identifying the percentage of atoms that make up the compounds.

#### **The water solubility test**

First, 10 mg of HNTs-Ag NPs and HNTs-FA-Ag NPs were poured into 15-mL flasks containing 2.5 mL of distilled water and 2.5 mL of toluene (Mo et al. 2021). The samples were put on the orbital shaker to shake for 2 h, then put inside the fixed stand and the changes in the shift of the samples towards the aqueous solvent were recorded after 10 min.

#### **Cell viability assay by MTT protocol**

The common MTT method was used to check the cell viability rate of the HCT116 colon cancer cells exposed to HNTs-Ag NPs and HNTs-FA-Ag NPs. For this purpose, the cells were cultured in a suitable culture medium and then transferred to 96-well plates at a density of  $1.3 \times 10^4$  cells per well (Sorinezami et al. 2019; Xu et al. 2023). Subsequently, the cells were treated with 8 different concentrations of HNTs-Ag NPs and HNTs-FA-Ag NPs (0.0188 mg/mL to 2.4 mg/mL), and after 48 and 72 h the cell viability was checked by the common MTT protocol. For each concentration, three repetitions ( $n=3, \pm$ SD) were considered to minimize the error. Additionally, *Acacia luciana* flower extract and cisplatin were introduced to HCT116 cancer cells to compare the results with those

obtained from modified HNTs. To conduct this experiment, freeze-dried flower extract was utilized, and concentrations similar to surface-modified HNTs were selected, ranging from 0.0188 mg/mL to 2.4 mg/mL for a meaningful comparison. Cisplatin, serving as a positive control, was tested at 8 different concentrations, ranging from 0.0188 mg/mL to 2.4 mg/mL, and exposed to cancer cells for 48 and 72 h. In both time periods of 48 and 72 h, three wells were designated as controls, in which the cells were not exposed to any combination. An incubator set at a temperature of 37 °C, a humidity level of 95%, and a CO<sub>2</sub> level of 5% was utilized during both the cultivation and cytotoxicity testing phases.

**Cell viability assay by sulforhodamine B**

For this purpose, HCT116 cells were transferred to a 96-well plate and incubated with 8 different concentrations of HNTs-Ag NPs and HNTs-FA-Ag NPs similar to the MTT method for 72 h at 37 °C. To start the process, first, the culture medium was removed from the wells, then 100 µL of cold 10% TCA was added to the wells and kept in the refrigerator (4 °C and away from light) for 60 min. Immediately, the excess TCA was washed and removed from the wells with sterile distilled water, and the wells were dried well by gentle air blowing. In the next step, 100 µL of 0.5% SRB solution was added to the wells and they were incubated again for half an hour in the dark and normal room temperature. Excess SRB was dissolved with 0.5% acetic acid solution and the wells were dried by gentle air blowing. Finally, 200 µL of Tris base (10 mM) was added to the wells and shaken for 20 min, and the absorbance of the pink-stained cells was read at 510 nm.

**Investigating the expression of genes involved in apoptosis by real-time PCR method**

Three separate flasks containing one million HCT116 colon cells were prepared, so that one of them was treated with 0.12 mg/mL of HNTs-Ag NPs, another with 7.6 × 10<sup>-4</sup> mg/mL of HNTs-FA-Ag NPs, and the last one was considered as a control. Concentrations of modified HNTs were selected based on IC<sub>50</sub> and the cells were incubated for 12 h. Then the treated cells were washed with PBS (2×), separated from the bottom of the flasks by trypsin, and collected by centrifugation (5 min at 4000 rpm). After re-suspending

**Table 1** Shows the genes used in this research, along with their corresponding sequences

| Genes              | Sequences  |
|--------------------|--|
| GAPDH <sup>a</sup> | F: TTGCCATCAATGACCCCTTCA<br>R: CGCCCCACTTGATTTTGGA   |
| AKT1               | F: CCAACACCTTCATCATCCGC<br>R: AGTCCATCTCCTCCTCTCC    |
| BAK1               | F: TCTGGGACCTCCTTAGCCCT<br>R: AATGGGCTCTCACAAGGGTATT |
| TLR6               | F: GCATTTCCAAGTCGTTTCTA<br>R: GCAAAAACCTTCACCTTGT    |
| Caspase-3          | F: TGCAGTCATTATGAGAGGCAAT<br>R: AAGTTTGAGCCTTTGACCA  |
| Bclx               | F: TGGAAAGCGTAGACAAGGAGA<br>R: TGCTGCATTGTTCCCATAGA  |

<sup>a</sup>The GAPDH gene was utilized as a housekeeping gene to normalize CT values

the cells in PBS, RNA isolation was performed by the High Pure RNA Isolation Kit, and the detailed steps were well described in our previous works (Sargazi et al. 2020; Habibi Khorassani et al. 2021; He et al. 2021). The cDNA synthesis kit was used for cDNA synthesis according to previous work (Dou et al. 2022). The expression of Bak1, Bclx, Caspase-3, and AKT1 genes was evaluated by Real-time PCR according to a special thermal cycle for these genes by the Applied Biosystems StepOne™ device (Thermo Fisher Scientific, Massachusetts, USA) (Sargazi et al. 2020). Table 1 shows the sequence of the mentioned genes.

#### **Lipid peroxidation assay in erythrocytes**

About 200 mL of heparinized blood was obtained from Zabol Blood Transfusion Organization, then it was centrifuged ( $2\times$ ) at 3000 rpm for half an hour to separate pure erythrocytes from the blood (Zhang and Heidari 2023). In the next step, the pure erythrocytes were washed ( $2\times$ ) with PBS and a mixture of 1:9 was prepared from erythrocytes and PBS, respectively. Using this erythrocyte mixture, four different concentrations (0.125, 0.25, 0.5, and 1 mg/mL) of HNTs-Ag NPs and HNTs-FA-Ag NPs were prepared with a final volume of 5 mL and incubated at 37 °C for 24h. At time intervals of 0 and 24 h, 1 mL was removed from each of the samples and added to the mixture of 2:1 trichloroacetic acid (20%) and thiobarbituric acid (0.028 M) and incubated at 100 °C for 15 min. Then the supernatant was separated by centrifugation and its absorbance was measured at a wavelength of 532 nm to obtain the amount of malondialdehyde (MDA) produced by erythrocytes. All steps were repeated three times to eliminate possible errors ( $n=3$ ).

#### **Investigating the amount of inflammation caused in erythrocytes by real-time PCR**

According to the previous protocol (Majd and Guo 2023), RNA was extracted from  $5\times 10^5$  erythrocytes treated with 0.12 mg/mL of HNTs-Ag NPs and  $7.6\times 10^{-4}$  mg/mL of HNTs-FA-Ag NPs. Subsequently, cDNA synthesis was performed, followed by checking the expression level of the TLR6 gene using real-time PCR.

## **Results and discussion**

### **Optimization and characterization of modified HNTs**

The unique hollow tubular structure of HNTs (interlayer and intracavity) plus their modifiable surface have made them widely used in drug delivery (Satish et al. 2019). The compatibility, good physicochemical properties, naturalness, and excellent solubility (Luo et al. 2020) made us decide to use HNTs as carriers of Ag NPs to improve their solubility and performance as well as reduce side effects. Accordingly, for the first time, two types of silver-HNTs drug delivery systems (HNTs-Ag NPs and HNTs-FA-Ag NPs) were synthesized to deliver Ag NPs to HCT116 colon cancer cells using FA. Accordingly, we modified the surface of HNTs using FA as a targeting agent and decorated it with green-synthesized Ag NPs as an anticancer agent. The surface modification agent was APTES to introduce amine groups onto the surface of HNTs (Karade et al. 2021) so we could conjugate the FA through an amide bond. We also used the green synthesis method to prepare Ag NPs using the *Acacia luciana* flower extract. It is mentioned in all the sources that the outer surface charge of HNTs is naturally negative and therefore, the  $\text{Ag}^+$  ions in the silver nitrate solution can be electrostatically attracted to this negative

charge (Masoud et al. 2023). One of the signs of the formation of Ag NPs on the surface of HNTs is the change in the color of the initial solution after adding *Acacia luciana* flower extract. The initial color of the solution containing HNTs and  $\text{Ag}^+$  ions was colorless and the initial color of the solution containing HNTs-FA and  $\text{Ag}^+$  ions was yellow, which changed to a dark brown after adding the reducing agent. Due to the presence of terpenoids and other hydrocarbons such as phytol acetate, linalool acetate, manool, etc. (Sardashti et al. 2015), *Acacia luciana* flowers extract can play a reducing role and convert  $\text{Ag}^+$  ions on the surface of modified HNTs into Ag NPs.

During the flowering months of April and October for *Acacia luciana* trees, it was discovered that flowers harvested in April contain a higher amount of extract. Different amounts of *Acacia luciana* flower powder (2, 5, 10, and 15 g) were dissolved in 100 mL of 40%, 50%, and 60% ethanol and shaken for 1 to 7 days. The most efficient extraction was achieved with 10 g in 100 mL of 60% ethanol after 3 days. Various amounts of silver nitrate and *Acacia luciana* extract (30, 40, 50, and 60 mg) were mixed with 100 mg of HNTs and HNTs-FA. The temperature ranged from 30 to 70 °C. The optimal condition was found to be an equal ratio of 50 mg of both compounds at a temperature of 50 °C.

Based on the efficiency and weight of the obtained products, it can be estimated that approximately 55 to 63% loading of Ag NPs onto the surface of HNTs has been successfully achieved. This loading can consist of both Ag NPs and flower extract biomolecules. It is not possible to detect the amounts of each of them individually. At each step, an FT-IR spectrum was taken to confirm the functional groups present in the surface modifications of HNTs. In addition to the absorptions related to HNTs, which can be seen in the FT-IR spectrum of Fig. 1A such as bands at 470, 1033, and 1090  $\text{cm}^{-1}$  associated with the Si–O vibrations, bands at 910, 3626, and 3695  $\text{cm}^{-1}$  related to the vibrations of the OH groups of the inner surface of HNTs, and band at 540  $\text{cm}^{-1}$  attributed to the Al–O vibration, several bands can be seen as indicator of HNTs-Ag NPs formation. For

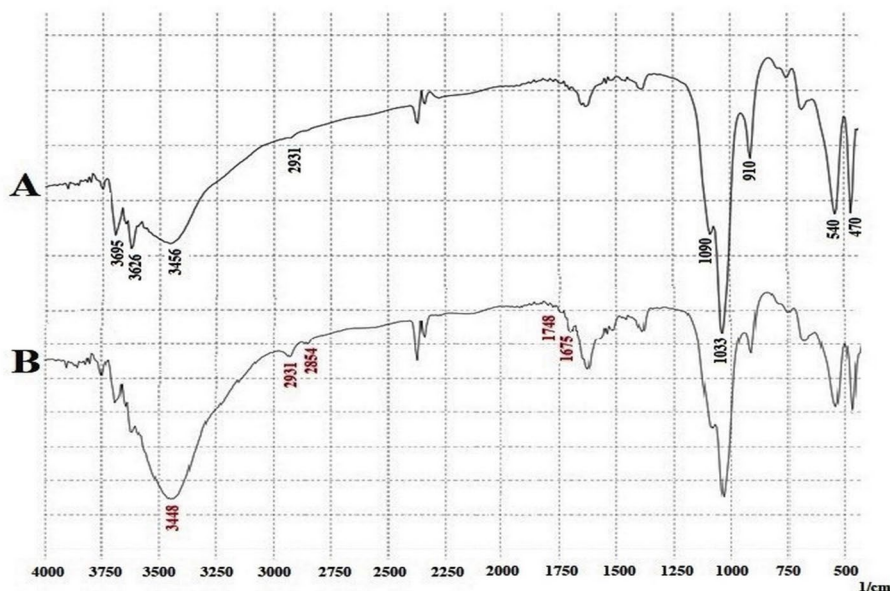


**Fig. 1** FT-IR spectra of **A** HNTs-Ag NPs and **B** HNTs-FA-Ag NPs. The spectra were taken in KBr with a resolution of 16  $\text{cm}^{-1}$

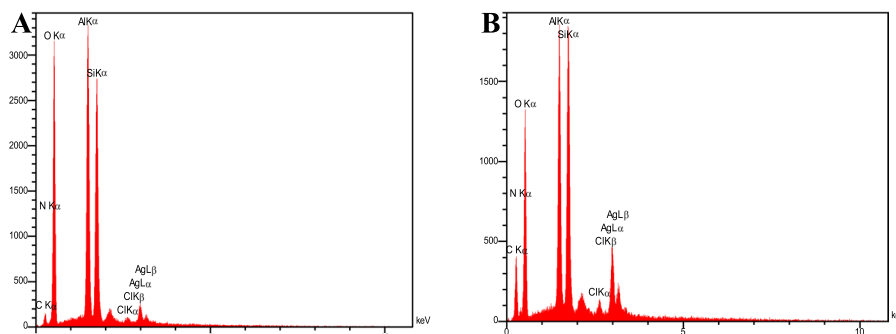


**Fig. 2** EDX diagram of **A** HNTs-Ag NPs and **B** HNTs-FA-Ag NPs

**Table 2** Displays the weight percentage and intensity of peaks associated with nanoparticles

| Elements of HNTs-Ag NPs | Intensity | Weight % | Elements of HNTs-FA-Ag NPs | Intensity | Weight % |
|-------------------------|-----------|----------|----------------------------|-----------|----------|
| Carbon                  | 27.4      | 11.05    | Carbon                     | 76.1      | 25.34    |
| Nitrogen                | 8.1       | 3.24     | Nitrogen                   | 11.3      | 6.59     |
| Oxygen                  | 540.3     | 55.96    | Oxygen                     | 243.0     | 40.80    |
| Aluminum                | 695.6     | 13.32    | Aluminum                   | 406.8     | 8.52     |
| Silica                  | 605.3     | 12.00    | Silica                     | 450.6     | 9.36     |
| Chlorine                | 20.6      | 0.52     | Chlorine                   | 20.1      | 0.54     |
| Silver                  | 60.3      | 3.90     | Silver                     | 127.0     | 8.85     |
|                         |           | 100.00   |                            |           | 100.00   |

example, the bands in 2854 and 2931  $\text{cm}^{-1}$  related to the stretching vibrations of  $\text{CH}_2$  groups of biomolecules of *Acacia luciana* flowers extract or the fingerprint region below 750  $\text{cm}^{-1}$  attributed to Ag NPs on the surface of modified HNTs. Of course, biomolecules also have OH groups, which created a strong absorption band in the 3456  $\text{cm}^{-1}$ .

In the spectrum related to HNTs-FA-Ag NPs (Fig. 1B), in addition to the presence of peaks related to HNTs-Ag NPs, the peak of the 3448  $\text{cm}^{-1}$  region has become wider, which is related to the stretching vibrations of hydroxyl groups FA and flower extract biomolecules. Also, the peaks of the 2854 and 2931  $\text{cm}^{-1}$  regions have become sharper, which is due to the increase in the number of methylene groups. In addition, absorption bands at 1675 and 1748  $\text{cm}^{-1}$  clearly prove the existence of carbonyl groups of FA (amide and carboxyl).

Another method that can confirm the correctness of the synthesis of modified HNTs is an elemental analysis by EDX. By comparing Fig. 2A and B, it is possible to understand the presence of biomolecules of flower extract, Ag NPs, an also FA. Basically, the building blocks of HNTs are included oxygen (O=61.6%), alumina (Al=8.2%), and silica (Si=20.2%) (Hebbar et al. 2017), but after decoration, additional peaks of carbon (C=11.05%), nitrogen (N=3.24%), and silver (Ag=3.9%) confirm the presence of Ag NPs on the surface of HNTs-Ag NPs (Fig. 2A). In addition, increasing the percentage of carbon (C=25.34%) and nitrogen (N=6.59%) (Fig. 2B) shows the good conjugation of FA to the HNTs. In addition, due to the increase in surface area, the percentage of silver

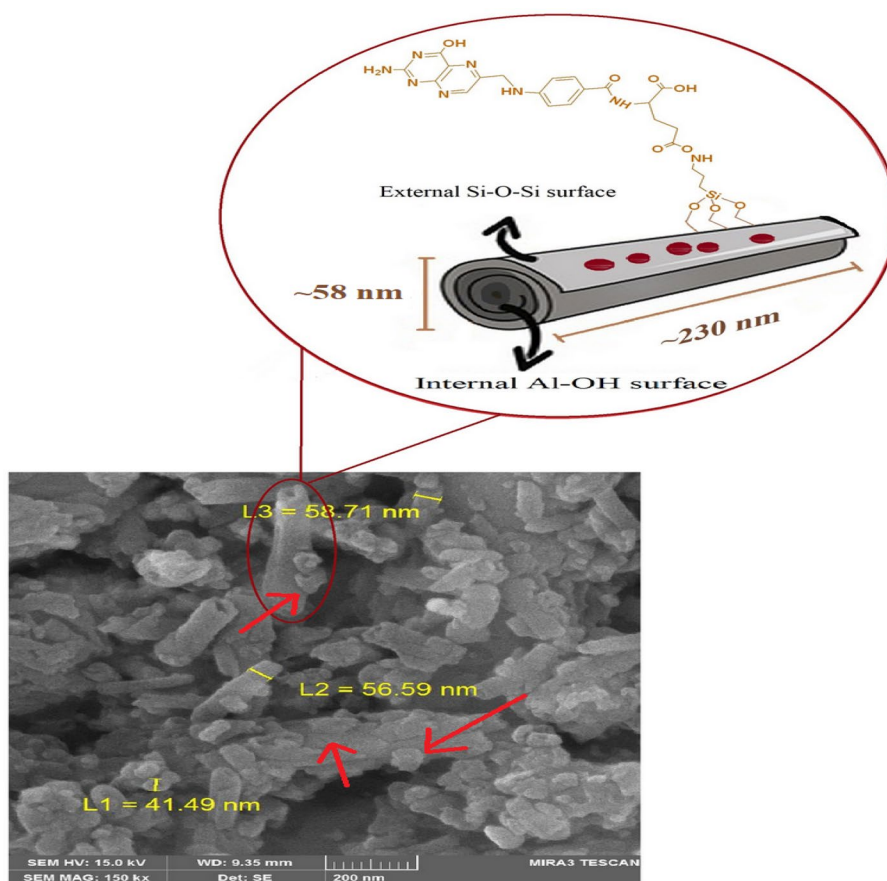


**Fig. 3** Using FESEM, the morphology of NPs was determined. The tubular structure of HNTs-FA-Ag NPs with a diameter of about 58 nm and a length of about 230 nm is quite evident. A number of groups attached to the surface of HNTs-FA-Ag NPs are marked by arrows, which can be related to Ag NPs and FA

(Ag=8.85%) has increased, which can be a reason for the presence of more Ag NPs on the surface of HNTs-FA-Ag NPs.

The increase in the intensity of the carbon, nitrogen, and silver peaks related to HNTs-FA-Ag NPs compared to HNTs-Ag NPs indicates the presence of folic acid and an increase in the loading of silver nanoparticles, as shown in Table 2.

The tubular structure of HNTs, which consists of aluminol groups on inner surface and silicon groups on outer surface, allows us to conjugate FA on their surface. Using FESEM, the tubular morphology of HNTs-FA-Ag NPs was found in Fig. 3 which have an average diameter of 58 nm and an average length of 230 nm.

It has already been confirmed that HNTs in the pH range of 5 to 8 have a negative charge of approximately  $-24$  mV due to the presence of deprotonated silanol groups (Zhang and Heidari 2023; Katana et al. 2020). As a result, they can attract positive silver ions on the outer surface. After the addition of *Acacia luciana* flower extract, the  $\text{Ag}^+$  ions directly turn into Ag NPs. To prove that Ag NPs are placed on the surfaces, we dissolved HNTs-Ag NPs in PBS with pH 7 and measured their zeta potential. Since Ag NPs have a slight negative charge due to biomolecules in the flower extract that help to reduce them, it was expected that the negative charge would increase somewhat. After measuring the zeta potential, it was found that the negative charge of the HNTs-Ag NPs

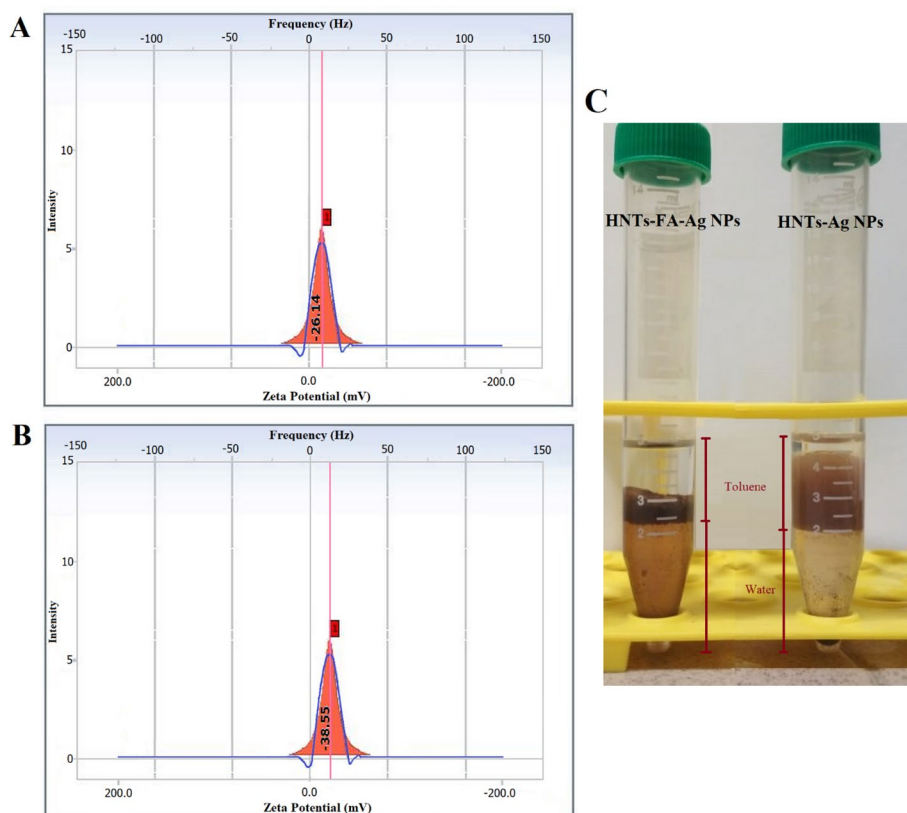


**Fig. 4** Surface potential of **A** HNTs-Ag NPs and **B** HNTs-FA-Ag NPs was measured by Malvern Zetasizer\_nanoZS. The presence of folic acid increases the negative charge on NPs. **C** Shows the better solubility of HNTs-FA-Ag NPs in water compared to HNTs-Ag NPs, so that in a short time, a significant amount of it penetrated the aqueous solvent

is about  $-26.14$  mV (Fig. 4A). Also, after the conjugation of FA to HNTs, the negative charge increased further and the zeta potential of HNTs-FA-Ag NPs was measured to be about  $-38.55$  mV (Fig. 4B). The increase in negative charge can be attributed to the carboxyl groups of FA that have been added to the surface of HNTs.

The role of zeta potential in the dispersity of NPs in aqueous solutions is very important because the NPs with likewise surface charges repel each other and electrostatically stabilize the particles in the solution (Pfeiffer et al. 2014). HNTs disperse well in water, especially after ultrasonication, which is obtained from the negative surface potential of HNTs in water (Pan et al. 2017). Therefore, we decided to measure the affinity of modified HNTs to the aqueous solvent, for this reason, we dissolved HNTs-Ag NPs and HNTs-FA-Ag NPs separately in toluene as an organic solvent and then placed them in the vicinity of the aqueous solvent. As can be seen in Fig. 4C, after 20 min, the HNTs-FA-Ag NPs penetrated a significant amount into the aqueous solvent, while the HNTs-Ag NPs showed less affinity for the aqueous solvent. The key point is the correlation between solubility in water and the values of zeta potential. This means that HNTs-FA-Ag NPs with a higher zeta potential value will penetrate and dissolve more effectively in the water solution. The reason for this can be attributed to the presence of carboxyl ions and the induction of a more negative charge in the HNTs-FA-Ag NPs. It has been

proven that the higher the zeta potential of a compound, the more uniformly it penetrates the aqueous solvent. This is due to repulsion between the charges, resulting in a larger amount being dissolved in the aqueous solvent (Malhotra and Coupland 2004).

**Measuring cell proliferation using MTT assay**

In the previous work, the effect of Ag NPs on a FR-positive cell line (MCF-7) was investigated and the IC<sub>50</sub> value of 4.37 mg/mL was calculated following 72 h of treatment (Sargazi et al. 2020). According to the size and morphology of the Ag NPs, as well as the biomolecules that are placed on their surface during green synthesis, Ag NPs can show a good effect on cancer cells (Alharbi and Alsubhi 2022). It has been proven that Ag NPs can passively enter cancer cells using enhanced permeability and retention (EPR) (Kalyane et al. 2019), and show their therapeutic effect. Of course, there is a concern that they cannot make a good distinction between cancer cells and normal cells and cause adverse effects (Gomes et al. 2021). Therefore, changing the size, solubility, and active targeting

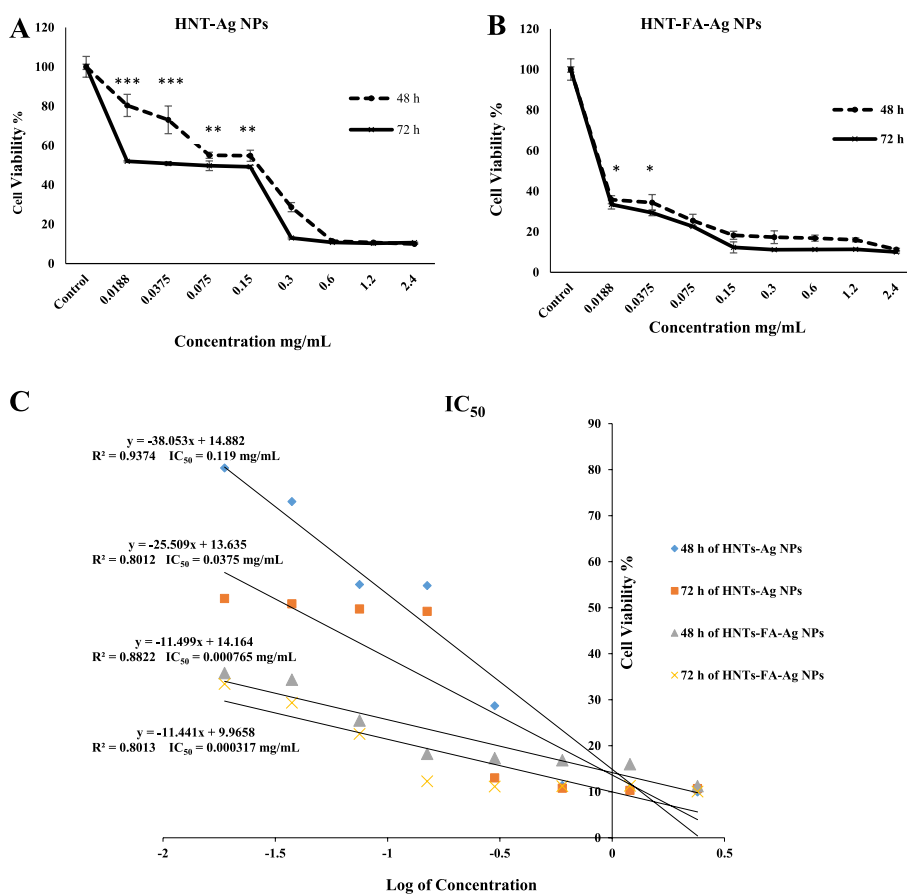


**Fig. 5** Cell survival assay of **A** HNTs-Ag NPs and **B** HNTs-FA-Ag NPs was performed using the MTT method. HNTs-FA-Ag NPs showed a good response at all concentrations and at both times. Panel **C** shows the IC<sub>50</sub> plot obtained based on the logarithm of concentrations versus cell viability %, and confirms that active targeting of FRs on HCT116 colon cancers by HNTs-FA-Ag NPs was well achieved. The data were analyzed using one-way analysis of variance (ANOVA) and Tukey's post hoc test, with a significance level set at P < 0.05

of cancer cells can increase the good performance of Ag NPs (Kovács et al. 2022). One way to change the size is to load Ag NPs on HNTs as a carrier agent. Also, by conjugating FA on HNTs and actively targeting cancer cells, the performance of Ag NPs on FR-positive cell line (HCT116) was investigated.

In our previous work, loading Ag NPs on HNTs and increasing the solubility by the nanotube carrier made Ag NPs able to show a very good therapeutic effect on floating leukemia cells (Zhang and Heidari Majd 2023). But in the present work, we went a step further and aimed to direct Ag NPs to cancer cells through active targeting by FRs. As it is clearly evident in Fig. 5, conjugation of FA on HNTs followed by active targeting showed a better effect on colorectal cells. Even at the lowest concentration, HNTs-FA-Ag NPs can control the cell viability to about 30% at both 48 and 72 h treatment, while HNTs-Ag NPs has a significant effect on cell viability at high concentrations. The IC<sub>50</sub> values in Fig. 5C confirm that HNTs-FA-Ag NPs can act more effectively than HNTs-Ag NPs by actively targeting FRs and stop the growth of HCT116 colon cancer cell lines in a concentration-dependent manner. The reason may be attributed to the active targeting of FRs by nanotubes containing folic acid. The overexpression of FRs on the surface of cancer cells makes FA a promising option for effective nano-drug delivery systems. It has been observed that enhanced entry through folate-mediated endocytosis results in a

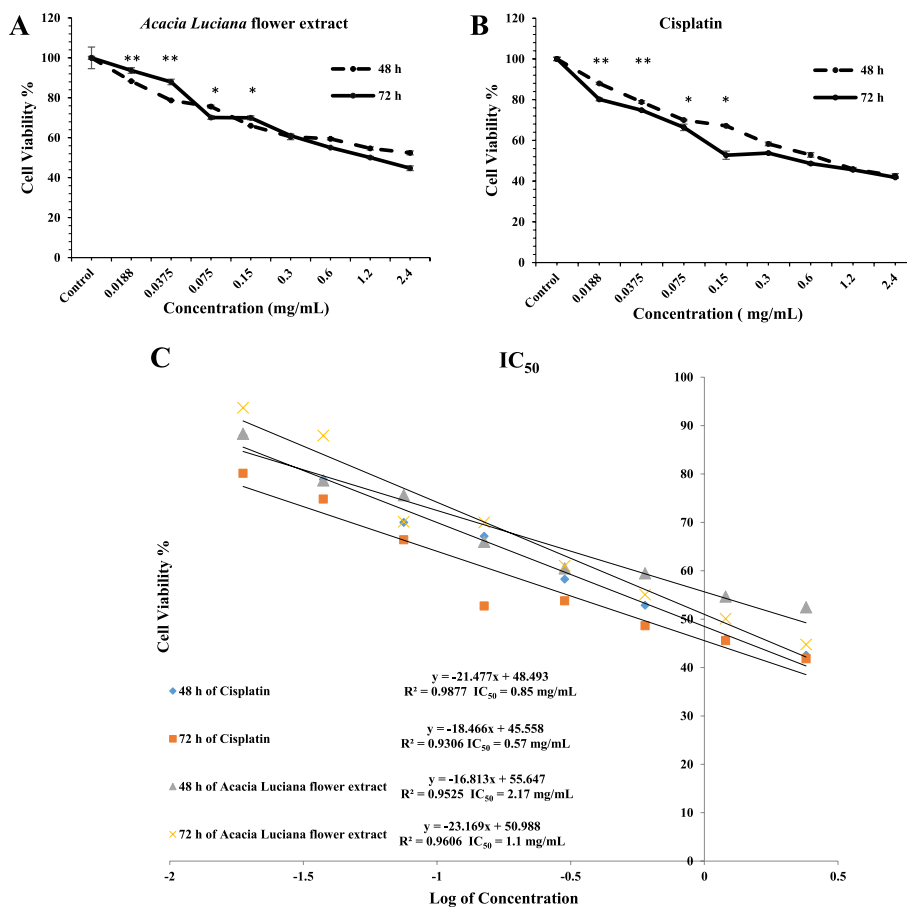


**Fig. 6** Cell survival assay of **A** *Acacia luciana* flower extract and **B** cisplatin was performed using the MTT method. Panel **C** shows IC<sub>50</sub> values. Significance level set at P < 0.05

155-fold decrease in the  $IC_{50}$  of the HNTs-FA-Ag NPs compared to the HNTs-Ag NPs after 48 h treatment (Fig. 5C). However, despite the increased size and lack of targeting agent, the cytotoxic effects of HNTs-Ag NPs on HCT116 cell lines are evident and can inhibit their growth at both 48 and 72 h.

A large percentage of chemical compounds identified in *Acacia luciana* flower extract are oxygenated monoterpenes (6.85%), sesquiterpene hydrocarbons (1.06%) and oxygenated diterpenes (50.8%) (Sardashti et al. 2015). To determine the impact of biomolecules in *Acacia luciana* flower extract, we conducted experiments exposing them to cancer cells for 48 and 72 h. The graph in Fig. 6A clearly illustrates that the flower extract only reduces cell viability to below 50% at a high concentration of 2.4 mg/mL after 72 h, with other concentrations proving ineffective. Linalool (Machado et al. 2022), manool (de Oliveira et al. 2016), geraniol (Cho et al. 2016), terpineol (Hassan et al. 2010), and feruginol (Shao et al. 2023) are among the most important biomolecules of *Acacia luciana* flower extract, whose anticancer properties have been proven. Comparing the  $IC_{50}$  value (Fig. 6C) to the  $IC_{50}$  values of HNTs (Fig. 5C), it can be inferred that when flower extracts are involved in the biosynthesis of green Ag NPs on halloysites' surface, they perform better. These compounds have the ability to facilitate the biosynthesis of Ag NPs and can also be deposited on their surface. Additionally, due to the properties of NPs, they are better able to infiltrate tumors, generate ROS more effectively, and subsequently harm the mitochondria of cancer cells.

Interestingly, cisplatin demonstrates weaker efficacy in inducing cell death compared to both HNTs-Ag NPs and HNTs-FA-Ag NPs, only proving effective at high concentrations after 48 and 72 h of contact with HCT116 cells (Fig. 6B) (Majd 2024).

A statistical comparison was conducted on the resulting graph of  $IC_{50}$  values after 48 and 72 h of treatment to demonstrate that HNTs-FA-Ag NPs outperformed cisplatin. All values were multiplied by 1000 for better readability. Figure 7 clearly indicates

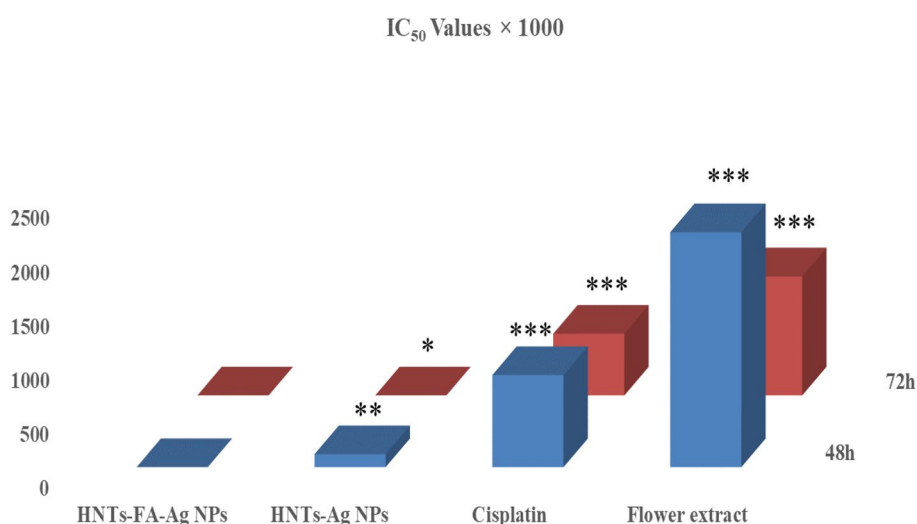


**Fig. 7** Statistical comparison was conducted on the  $IC_{50}$  results obtained from four combinations: HNTs-FA-Ag NPs, HNTs-Ag NPs, cisplatin, and *Acacia luciana* flower extract. All values were multiplied by 1000. The data were analyzed using one-way analysis of variance (ANOVA) and Tukey's post hoc test, with a significance level set at  $P < 0.05$

a significant difference between the IC<sub>50</sub> values of cisplatin and *Acacia luciana* flower extract with HNTs-FA-Ag NPs and HNTs-Ag NPs (P-value < 0.05), confirming that the modified HNTs exhibited strong performance in inhibiting colon cancer cell growth. These results also suggest that HNTs-FA-Ag NPs performed better than HNTs-Ag NPs.

**Measuring cell proliferation using SRB staining method**

Sometimes various environmental factors or the presence of some compounds cause the result of the MTT method to be wrong because the conversion of MTT to formazan by the cell is a kind of metabolic process and it may increase or decrease (Plumb et al. 1989). Therefore, we decided to check cell viability based on the protein content of cells and by SRB staining to ensure the ability of nanoparticles to inhibit cancer cells. As shown in Fig. 8A, both HNTs-Ag NPs and HNTs-FA-Ag NPs were able to inhibit HCT116 colon cancer cells and reduced the protein content of cancer cells, although HNTs-FA-Ag NPs showed better inhibition due to the presence of folic acid and active targeting of cancer cells. The obtained IC<sub>50</sub> value also confirms the greater ability of HNTs-FA-Ag NPs (Fig. 8B), although the values obtained from the SRB staining method are lower than the IC<sub>50</sub> values obtained from the MTT method, which is normal.

**Expression level of genes involved in apoptosis induction and apoptosis inhibition**

Research by the International Cancer Agency confirmed that colorectal cancer is the second most common cancer in women and the third most common cancer in men (Arnold et al. 2017). Since 5-fluorouracil is the only drug approved for the treatment of colon cancer (Kelly et al. 2013), it can be a great challenge for researchers and oncologists because it causes numerous side effects for the patient and increases the need for alternative treatment strategies (Kanterman et al. 2014). Various methods of investigating gene expression, including RT-PCR, fluorescence, and western blot, confirm that Ag NPs can induce apoptosis by increasing the production of ROS in mitochondria and splitting its membrane. On the other hand, independently of caspase and through the p53 gene, they can increase the amount of apoptosis (Varunkumar et al. 2020). Therefore, it can be concluded that Ag NPs induce apoptosis in both mitochondria-dependent and non-mitochondria-dependent ways (Gurunathan et al. 2013).

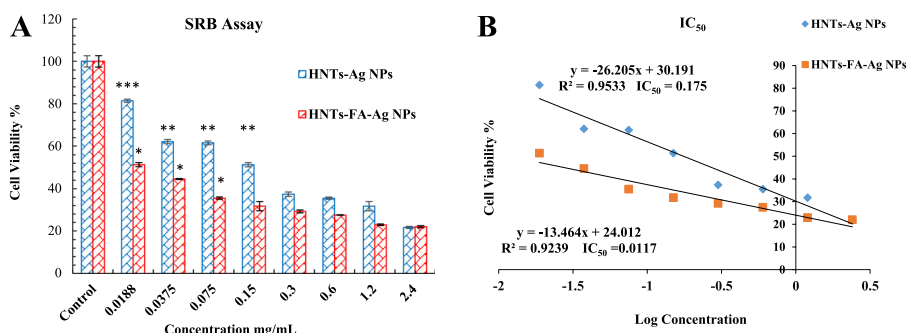


**Fig. 8** A Evaluation of inhibition of HCT116 cells treated with HNTs-Ag NPs and HNTs-FA-Ag NPs utilizing SRB staining method. B Calculation of IC<sub>50</sub> by plotting the logarithm of concentration versus cell viability %. Significance level set at P < 0.05

Since Ag NPs are available in two forms, HNTs-Ag NPs and HNTs-FA-Ag NPs, therefore, investigating the different pathways of apoptosis induction, including internal and external pathways, as well as the pathway of apoptosis inhibition, can provide a good perspective for the induction of apoptosis by Ag NPs. Changes in the expression of two proteins, Bax and Bcl-2, are very important because they can indicate mitochondrial damage when treated with modified HNTs. The increase in the ratio of Bax to Bcl-2 causes the release of Cyt-c and the formation of apoptosis protease activating factor 1 (Apaf-1), which indicates the induction of apoptosis from the mitochondrial-dependent intrinsic pathway (Siddiqui et al. 2015). To investigate the extrinsic pathway, caspase-3 gene expression can be examined, as cleavage of procaspase-9 directly activates caspase-3 and leads to cell death by apoptosis (Ahmadian et al. 2018). Gurunathan et al.'s research on HCT116 human colon cancer cells showed that Ag NPs significantly increased ROS production and MDA levels, causing mitochondrial dysfunction and inducing DNA damage in cells (Gurunathan et al. 2018). Since the positive effect of bio-synthesized Ag NPs by *Acacia luciana* flower extract on the regulation of Bak1 and Bclx genes was proven (Sargazi et al. 2020), we decided to load Ag NPs on modified HNTs and measure the effect of size change and active targeting on gene expression. On the other hand, we decided to investigate the expression of AKT1 gene to investigate the possibility of resistance to treatment or inhibition of apoptosis due to its specific structure and the presence of HNTs as nanocarriers. One common sign of resistance to conventional chemotherapy drugs and other biological agents used in cancer treatment is the abnormal activation of the PI3K/AKT pathway (Fruman et al. 2017). This activation leads to an increase in the expression of the AKT1 gene (Hasbal-Celikok et al. 2021).

The results of Fig. 9 show that the presence of folic acid in the structure of HNTs-FA-Ag NPs was able to increase the expression of the Bak1 gene more than the control

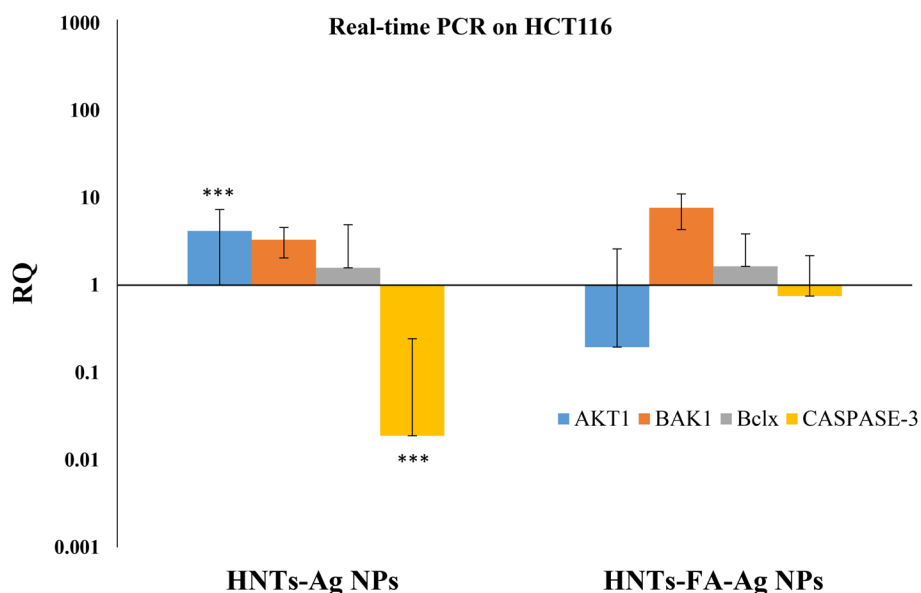


**Fig. 9** Shows the expression levels of genes involved in apoptosis and treatment resistance. Each sample was assayed in duplicate, and the average cycle threshold (CT) value was normalized to the housekeeping gene GAPDH. The fold change expression was calculated using the  $\Delta\Delta CT$  method, where RQ equals  $2^{-\Delta\Delta CT}$ . The middle line represents 1 and indicates the expression level of the control. Significance level set at  $P < 0.05$

and even HNTs-Ag NPs. In a research conducted by Cao et al., it was confirmed that treatment with folic acid plays an important role in the chemical prevention of gastric cancer (Cao et al. 2005) so the expression of tumor suppressor p53 gene in the gastric mucosa increases significantly after its use. Also, Attias et al. confirmed that folic acid causes a dose-dependent reduction of IGF-IR protein in HCT116 colon cancer cells in a p53-dependent manner, while it has no effect in wild-type p53-depleted HCT116 cells (Attias et al. 2006). Since the increase in p53 gene expression is directly related to the increase in Bak1 gene expression (Ramadan et al. 2019), it can be concluded that folic acid plays a role in the activation of the mitochondrial intrinsic pathway and increases Bak1 gene expression by HNTs-FA-Ag NPs subsequently, the Bak1/Bclx ratio becomes 4.71 times higher than the control.

As previously mentioned, one of the ways to detect the extrinsic pathway of apoptosis is to check the level of caspase-3 gene expression when the cancer cells are treated with modified HNTs (Cullen and Martin 2009). The results in Fig. 9 show that both HNTs-FA-Ag NPs and HNTs-Ag NPs could not promote apoptosis through this pathway and did not change the expression of the caspase-3 gene. According to the research conducted by Jahani-Asl et al. (2007), we expected that the pattern of AKT1 cleavage and inactivation depends on caspase-3 activity, and therefore, due to the decrease in caspase-3 expression, AKT1 protein expression increases. However, HNTs-FA-Ag NPs decreased the expression of the AKT1 gene by 0.197 compared to the control, while HNTs-Ag NPs could not decrease the expression of the AKT1 gene as predicted.

It was found in several studies that folic acid can prevent the expression of AKT proteins (Bhanumathi et al. 2018). For example, Wang et al. treated breast cancer cells (MDA-MB-231) with folate and observed that folic acid inhibited the growth of MDA-MB-231 cells and inhibited the expression of Bcl-2, and p-AKT proteins while increasing the expression of Bax, PTEN, and P53 proteins (Wang et al. 2020). Since AKT1 is a cellular response protein and can cause cell survival and resistance to tumor treatment (Los et al. 2009), so inhibiting its expression can help cure cancer and prevent cancer metastasis. Therefore, the reduction of AKT1 expression by HNTs-FA-Ag NPs can be attributed to the presence of folic acid in its structure, which makes Ag NPs perform better in inhibiting metastases of HCT116 colon cancer cell lines, while HNTs-Ag NPs lack such ability. In a similar study, Bhanumathi et al. synthesized an FA-PEG@BBR-AgNP drug delivery system containing folic acid, berberine, polyethylene glycol, and Ag NPs (Bhanumathi et al. 2018). They proved that this system can be useful as a therapeutic agent for MDA-MB-231 breast cancer as it can reduce the expression of cellular response proteins like AKT, Ras, Raf, PI3K, and ERK and increase the expression of apoptosis proteins like caspase-3, caspase-9, and Bax.

#### **Investigate the adverse effect of exposure to modified HNTs in erythrocytes**

Exogenous compounds that enter the bloodstream as drugs or drug carriers may be harmful to different blood cells like platelets, granulocytes, and erythrocytes (Pham-Huy et al. 2008). Meanwhile, NPs may cause cytotoxicity and oxidative stress in erythrocytes due to their special structure, function and size (Abbasi et al. 2023). It has been proven that nano-sized particles are usually more toxic than larger-sized compounds (Nel et al. 2006), for example, when Ag NPs enter the body of living organisms, they may interact

with different tissues and produce oxidative stress due to the release of Ag<sup>+</sup> ions (Kim et al. 2009). To all these points, the excessive vulnerability of red blood cells against oxidative stress due to the lack of a nucleus and endoplasmic reticulum to replace damaged proteins should also be added (Maurya et al. 2015).

The hypothesis is that NPs prepared through green synthesis can control the formation of free radicals due to being reduced by various plant biomolecules that contain large amounts of alkaloid, phenolic, terpenoid, flavonoid, glycoprotein, etc., compounds and eliminate oxidative stress (Kuppusamy et al. 2016). Since the *Acacia luciana* flower extract used to prepare HNTs-Ag NPs and HNTs-FA-Ag NPs contains large amounts of active molecules (Sardashti et al. 2015), it can be expected that they have little adverse effects on erythrocytes.

Also, after loading Ag NPs on HNTs, the size and solubility in the biological environment increased, which can help to reduce the side effects. The usual method for evaluating oxidative stress is to check the amount of MDA production by lipid peroxidation of unsaturated fatty acids (Tsikas 2017), the results of which are seen in Fig. 10. The graphs show that erythrocytes can increase the amount of MDA compared to the control only at the initial moments (time 0) of exposure to both HNTs-Ag NPs and HNTs-FA-Ag NPs and with their two high concentrations, while after 24 h, all concentrations decreased MDA production and showed protective effects (Fig. 10A and B).

Statistical comparison shows that only at the beginning of the test ( $t=0$ ), HNTs-Ag NPs at a concentration of 1 mg/mL and HNTs-FA-Ag NPs at two concentrations of 0.5 and 1 mg/mL have significantly increased MDA production ( $P$ -value < 0.05). Other concentrations did not cause oxidative stress on erythrocytes. Therefore, it is hoped that long-term exposure of modified HNTs to erythrocytes will not cause any complications, including lipid peroxidation. In fact, it may even have a protective effect and reduce oxidative stress. The reason for the decrease in lipid peroxidation of modified HNTs can be related to the larger size, increased solubility of Ag NPs, specific receptor targeting, and anti-inflammatory properties of HNTs. In the previous work, it was proved that increasing the solubility and increasing the size of Ag NPs by HNTs can have inhibitory effects on lipid peroxidation and prevent damage to erythrocytes (Zhang and Heidari Majd 2023). Also, Cornejo-Garrido et al. confirmed that HNTs as a natural and biocompatible carrier can show protective effects and reduce the production of nitric oxide to inhibit oxidative stress (Cornejo-Garrido et al. 2012).

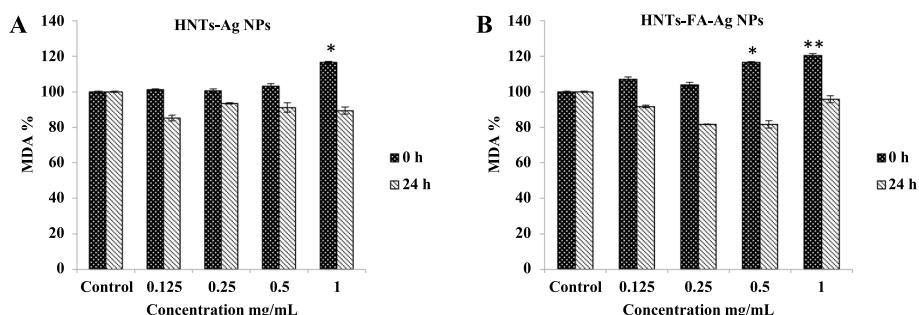


**Fig. 10** Evaluation of MDA production by erythrocytes after exposure to **A** HNTs-Ag NPs and **B** HNTs-FA-Ag NPs. One-way analysis of variance (ANOVA) and Tukey's post hoc test ( $P$ -value < 0.05) were used to analyze and estimated the data ( $n = 3, \pm SD$ )

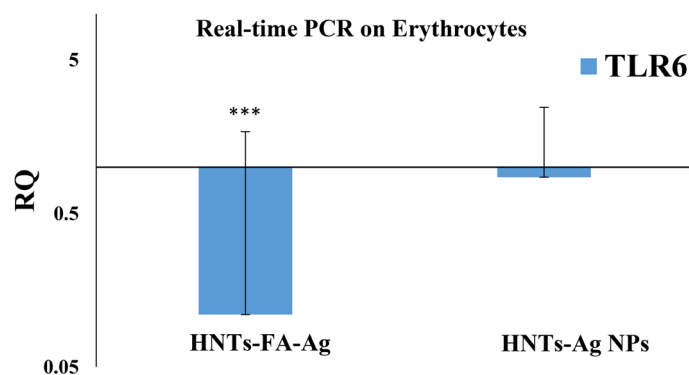


**Fig. 11** Shows the TLR6 gene expression after a 24-h exposure of HNTs-Ag NPs and HNTs-FA-Ag NPs to erythrocytes. Significance level set at  $P < 0.05$

### Examining the level of inflammation through real-time PCR

After confirming the possible protective role of HNTs in reducing oxidative stress and damage to erythrocytes, we decided to investigate the inflammatory response of blood cells when in contact with HNTs-Ag NPs and HNTs-FA-Ag NPs. The TLR6 gene plays a role in intensifying the inflammatory response associated with tissue damage following exposure to exogenous compounds in close proximity to body cells. TLRs activate the immune system by regulating the activation of antigen-presenting cells and key cytokines (Duan et al. 2022).

As seen in Fig. 11, both modified HNTs did not initiate any inflammatory response in erythrocytes and did not increase TLR6 gene expression. The noteworthy point is the better effect of HNTs-FA-Ag NPs, which can be attributed to the presence of folic acid. This is consistent with the results of AKT1 gene expression, which indicated that the presence of FA reduces resistance to treatment.

### Conclusion

In this research, for the first time, halloysite nanotubes (HNTs) loaded with silver nanoparticles (Ag NPs) and folic acid (FA) were synthesized to target HCT116 colon cancer cells, which overexpress FRs. The MTT assay and SRB staining method confirmed that HNTs-FA-Ag NPs reduced cell viability in a concentration-dependent manner. Real-time PCR analysis showed that the presence of FA in the structure of HNTs-FA-Ag NPs activated the mitochondrial intrinsic pathway in HCT116 cells, increasing the Bak1/Bclx ratio compared to the control. Additionally, it significantly decreased the expression of AKT1, a protein responsible for cell survival and treatment resistance. Furthermore, both HNTs-Ag NPs and HNTs-FA-Ag NPs exhibited protective effects on erythrocytes, reduced oxidative stress after 24 h of exposure, and prevented inflammation in cells. Therefore, it is hopeful that HNTs-FA-Ag NPs can enhance the therapeutic effects of green Ag NPs and minimize their side effects.

### Acknowledgements

The authors would like to thank the Deputy of Research and Technology at Zabol University of Medical Sciences for their support.

### Author contributions

In order to acknowledge each author's contributions, we would like to highlight the following: MHM contributed to designing, writing, laboratory work, and editing. KBM collaborated in editing the text and conducting additional

tests. HW designed the study and supervised the experiments. All authors made substantial contributions to the final manuscript and have approved its submission. They are also aware of the order of authorship and have approved the submitted version of the manuscript.

#### Funding

Not applicable.

#### Data availability

No datasets were generated or analysed during the current study.

#### Declarations

##### Ethics approval and consent to participate

The content of this manuscript was reviewed by the ethics committee of Zabol University of Medical Sciences and approved with the ethics code IR.ZBMU.REC.1400.106. There were no participants in this research.

##### Consent for publication

Not applicable.

##### Competing interests

The authors declare no competing interests.

Received: 14 May 2024 Accepted: 23 January 2025

Published online: 16 February 2025

#### References

- Abbasi R, Shineh G, Mobaraki M, Doughty S, Tayebi L (2023) Structural parameters of nanoparticles affecting their toxicity for biomedical applications: a review. *J Nanopartic Res* 25(3):43
- Ahmadian E, Dizaj SM, Rahimpour E, Hasanzadeh A, Eftekhari A, Hosain Zadehan H et al (2018) Effect of silver nanoparticles in the induction of apoptosis on human hepatocellular carcinoma (HepG2) cell line. *Mater Sci Eng C Mater Biol Appl* 93:465–471
- Alharbi NS, Alsubhi NS (2022) Green synthesis and anticancer activity of silver nanoparticles prepared using fruit extract of *Azadirachta indica*. *J Radiat Res Appl Sci* 15(3):335–345
- Arnold M, Sierra MS, Laversanne M, Soerjomataram I, Jemal A, Bray F (2017) Global patterns and trends in colorectal cancer incidence and mortality. *Gut* 66(4):683–691
- Attias Z, Werner H, Vaisman N (2006) Folic acid and its metabolites modulate IGF-I receptor gene expression in colon cancer cells in a p53-dependent manner. *Endocr Relat Cancer* 13(2):571–581
- Bhanumathi R, Manivannan M, Thangaraj R, Kannan S (2018) Drug-carrying capacity and anticancer effect of the folic acid- and berberine-loaded silver nanomaterial to regulate the AKT-ERK pathway in breast cancer. *ACS Omega* 3(7):8317–8328
- Cao DZ, Sun WH, Ou XL, Yu Q, Yu T, Zhang YZ et al (2005) Effects of folic acid on epithelial apoptosis and expression of Bcl-2 and p53 in premalignant gastric lesions. *World J Gastroenterol* 11(11):1571–1576
- Cheng C, Song W, Zhao Q, Zhang H. Halloysite nanotubes in polymer science: purification, characterization, modification and applications. 2020;9(1):323–44.
- Cho M, So I, Chun JN, Jeon JH (2016) The antitumor effects of geraniol: modulation of cancer hallmark pathways (Review). *Int J Oncol* 48(5):1772–1782
- Cornejo-Garrido H, Nieto-Camacho A, Gómez-Vidales V, Ramírez-Apan MT, del Angel P, Montoya JA et al (2012) The anti-inflammatory properties of halloysite. *Appl Clay Sci* 57:10–16
- Cullen SP, Martin SJ (2009) Caspase activation pathways: some recent progress. *Cell Death Differ* 16(7):935–938
- de Oliveira PF, Munari CC, Nicolella HD, Veneziani RC, Tavares DC (2016) Manool, a *Salvia officinalis* diterpene, induces selective cytotoxicity in cancer cells. *Cytotechnology* 68(5):2139–2143
- Deng M, Chen P, Liu F, Fu S, Tang H, Fu Y et al (2012) The p53-Bak apoptotic signaling axis plays an essential role in regulating differentiation of the ocular lens. *Curr Mol Med* 12(8):901–916
- Dou J, Mi Y, Daneshmand S, Heidari MM (2022) The effect of magnetic nanoparticles containing hyaluronic acid and methotrexate on the expression of genes involved in apoptosis and metastasis in A549 lung cancer cell lines. *Arab J Chem* 15(12):104307
- Duan T, Du Y, Xing C, Wang HY, Wang RF (2022) Toll-like receptor signaling and its role in cell-mediated immunity. *Front Immunol* 13:812774
- Fruman DA, Chiu H, Hopkins BD, Bagrodia S, Cantley LC, Abraham RT (2017) The PI3K pathway in human disease. *Cell* 170(4):605–635
- Ganguly S, Bhawal P, Choudhury A, Mondal S, Das P, Das NC (2018) Preparation and properties of halloysite nanotubes/poly(ethylene methyl acrylate)-based nanocomposites by variation of mixing methods. *Polym-Plast Technol Eng* 57(10):997–1014
- Ghalei S, Hopkins S, Douglass M, Garren M, Mondal A, Handa H (2021) Nitric oxide releasing halloysite nanotubes for biomedical applications. *J Colloid Interface Sci* 590:277–289
- Gomes HIO, Martins CSM, Prior JAV (2021) Silver nanoparticles as carriers of anticancer drugs for efficient target treatment of cancer cells. *Nanomaterials*. <https://doi.org/10.3390/nano11040964>
- Gurunathan S, Han JW, Eppakayala V, Jeyaraj M, Kim JH (2013) Cytotoxicity of biologically synthesized silver nanoparticles in MDA-MB-231 human breast cancer cells. *Biomed Res Int* 2013:535796

- Gurunathan S, Qasim M, Park C, Yoo H, Kim JH, Hong K (2018) Cytotoxic potential and molecular pathway analysis of silver nanoparticles in human colon cancer cells HCT116. *Int J Mol Sci* 19(8):2269
- Habibi Khorassani SM, Ghodsi F, Arezomandan H, Shahrahi M, Omidikia N, Hashemzaei M, Heidari Majd M. In vitro apoptosis evaluation and kinetic modeling onto cyclodextrin-based host–guest magnetic nanoparticles containing methotrexate and tamoxifen. *BioNanoScience*. 2021.
- Hasbal-Celikok G, Aksoy-Sagirli P, Altiparmak-Ulbeği G, Can A (2021) Identification of AKT1/ $\beta$ -catenin mutations conferring cetuximab and chemotherapeutic drug resistance in colorectal cancer treatment. *Oncol Lett* 21(3):209
- Hassan SB, Gali-Muhtasib H, Göransson H, Larsson R (2010) Alpha terpineol: a potential anticancer agent which acts through suppressing NF- $\kappa$ B signalling. *Anticancer Res* 30(6):1911–1919
- He C, Heidari Majd M, Shiri F, Shahrahi S (2021) Palladium and platinum complexes of folic acid as new drug delivery systems for treatment of breast cancer cells. *J Mol Struct*. <https://doi.org/10.1016/j.molstruc.2020.129806>
- Hebbar RS, Isloor AM, Zulfhairun AK, Sohaimi Abdullah M, Ismail AF (2017) Efficient treatment of hazardous reactive dye effluents through antifouling polyetherimide hollow fiber membrane embedded with functionalized halloysite nanotubes. *J Taiwan Inst Chem Eng* 72:244–252
- Jahani-Asl A, Basak A, Tsang BK (2007) Caspase-3-mediated cleavage of Akt: Involvement of non-consensus sites and influence of phosphorylation. *FEBS Lett* 581(16):2883–2888
- Kalyane D, Raval N, Maheshwari R, Tambe V, Kalia K, Tekade RK (2019) Employment of enhanced permeability and retention effect (EPR): Nanoparticle-based precision tools for targeting of therapeutic and diagnostic agent in cancer. *Mater Sci Eng C Mater Biol Appl* 98:1252–1276
- Kanterman J, Sade-Feldman M, Biton M, Ish-Shalom E, Lasry A, Goldshtein A et al (2014) Adverse immunoregulatory effects of 5FU and CPT11 chemotherapy on myeloid-derived suppressor cells and colorectal cancer outcomes. *Cancer Res* 74(21):6022–6035
- Karade VC, Sharma A, Dhavale RP, Dhavale RP, Shingte SR, Patil PS et al (2021) APTES monolayer coverage on self-assembled magnetic nanospheres for controlled release of anticancer drug Nintedanib. *Sci Rep* 11(1):5674
- Karewicz A, Machowska A, Kasprzyk M, Ledwójcik G (2021) Application of halloysite nanotubes in cancer therapy—a review. *Materials (Basel)*. 14(11):2943
- Katana B, Takács D, Csapó E, Szabó T, Jamnik A, Szilagyi I (2020) Ion specific effects on the stability of halloysite nanotube colloids-inorganic salts versus ionic liquids. *J Phys Chem B* 124(43):9757–9765
- Kelly C, Bhuvana N, Harrison M, Buckley A, Saunders M (2013) Use of raltitrexed as an alternative to 5-fluorouracil and capecitabine in cancer patients with cardiac history. *Eur J Cancer* 49(10):2303–2310
- Kim S, Choi JE, Choi J, Chung KH, Park K, Yi J, Ryu DY (2009) Oxidative stress-dependent toxicity of silver nanoparticles in human hepatoma cells. *Toxicol Vitro* 23(6):1076–1084
- Kovács D, Igaz N, Gopisetty MK, Kiricsi M (2022) Cancer therapy by silver nanoparticles: fiction or reality? *IJMS*. <https://doi.org/10.3390/ijms23020839>
- Kuppusamy P, Yusoff MM, Maniam GP, Govindan N (2016) Biosynthesis of metallic nanoparticles using plant derivatives and their new avenues in pharmacological applications—an updated report. *Saudi Pharmaceutical Journal* 24(4):473–484
- Leamon CP, Reddy JA (2004) Folate-targeted chemotherapy. *Adv Drug Deliv Rev* 56(8):1127–1141
- Leibowitz B, Yu J (2010) Mitochondrial signaling in cell death via the Bcl-2 family. *Cancer Biol Ther* 9(6):417–422
- Li Q, Ren T, Perkins P, Hu X, Wang X (2021) Applications of halloysite nanotubes in food packaging for improving film performance and food preservation. *Food Control* 124:107876
- Los M, Maddika S, Erb B, Schulze-Osthoff K (2009) Switching Akt: from survival signaling to deadly response. *BioEssays* 31(5):492–495
- Luo Y, Humayun A, Murray TA, Kemp BS, McFarland A, Liu X, Mills DK (2020) Cellular analysis and chemotherapeutic potential of a bi-functionalized halloysite nanotube. *Pharmaceutics* 12(10):962
- Machado TQ, da Fonseca ACC, Duarte ABS, Robbs BK, de Sousa DP (2022) A narrative review of the antitumor activity of monoterpenes from essential oils: an update. *Biomed Res Int* 2022:6317201
- Majd MH (2022) Dual-targeting and specific delivery of tamoxifen to cancer cells by modified magnetic nanoparticles using hyaluronic acid and folic acid. *Tumor Discovery* 1(1):1–9
- Majd MH (2024) Combination therapy of cisplatin and green silver nanoparticles enhances cytotoxicity and apoptosis in breast cancer cells. *CP*. <https://doi.org/10.36922/cp.2770>
- Majd MH, Guo X (2023) Investigation of the apoptosis inducing and  $\beta$ -catenin silencing by tetradentate schiff base zinc(II) complex on the T-47D breast cancer cells. *Anticancer Agents Med Chem* 23(15):1740–1746
- Malhotra A, Coupland JN (2004) The effect of surfactants on the solubility, zeta potential, and viscosity of soy protein isolates. *Food Hydrocolloids* 18(1):101–108
- Masoud A-R, Alakija F, Perves Bappy MJ, Mills PAS, Mills DK (2023) Metallizing the surface of halloysite nanotubes—a review. *Coatings* 13(3):542
- Maurya PK, Kumar P, Chandra P (2015) Biomarkers of oxidative stress in erythrocytes as a function of human age. *World J Methodol* 5(4):216–222
- Mo X, Wu F, Li Y, Cai X (2021) Hyaluronic acid-functionalized halloysite nanotubes for targeted drug delivery to CD44-overexpressing cancer cells. *Mater Today Commun* 28:102682
- Muntané J (2011) Harnessing tumor necrosis factor receptors to enhance antitumor activities of drugs. *Chem Res Toxicol* 24(10):1610–1616
- Nel A, Xia T, Mädler L, Li N (2006) Toxic potential of materials at the nanolevel. *Science* 311(5761):622–627
- Pan Q, Li N, Hong Y, Tang H, Zheng Z, Weng S et al (2017) Halloysite clay nanotubes as effective nanocarriers for the adsorption and loading of vancomycin for sustained release. *RSC Adv* 7(34):21352–21359
- Pfeiffer C, Rehbock C, Hühn D, Carrillo-Carrion C, de Aberasturi DJ, Merk V et al (2014) Interaction of colloidal nanoparticles with their local environment: the (ionic) nanoenvironment around nanoparticles is different from bulk and determines the physico-chemical properties of the nanoparticles. *J R Soc Interface* 11(96):20130931
- Pham-Huy LA, He H, Pham-Huy C (2008) Free radicals, antioxidants in disease and health. *Int J Biomed Sci* 4(2):89–96

- Plumb JA, Milroy R, Kaye SB (1989) Effects of the pH dependence of 3-(4,5-Dimethylthiazol-2-yl)-2,5-diphenyltetrazolium bromide-formazan absorption on chemosensitivity determined by a novel tetrazolium-based assay 1. *Can Res* 49(16):4435–4440
- Ramadan MA, Shawkey AE, Rabeh MA, Abdellatif AO (2019) Expression of P53, BAX, and BCL-2 in human malignant melanoma and squamous cell carcinoma cells after tea tree oil treatment in vitro. *Cytotechnology* 71(1):461–473
- Sardashti AR, Valizadeh J, Majd MH (2015) Chemical constituents of the flower oil of *Acacia luciana* from Iran. *Int J Agric Crop Sci* 8(3):395
- Sargazi A, Barani A, Heidari MM (2020) Synthesis and apoptotic efficacy of biosynthesized silver nanoparticles using acacia luciana flower extract in MCF-7 breast cancer cells: activation of Bak1 and Bclx for cancer therapy. *BioNano-Science* 10(3):683–689
- Satish S, Tharmavaram M, Rawtani D (2019) Halloysite nanotubes as a nature's boon for biomedical applications. *Nano-biomedicine* 6:1849543519863625
- Shao L, González-Cardenete MA, Prieto-García JM (2023) In vitro cytotoxic effects of ferruginol analogues in Sk-MEL28 human melanoma cells. *Int J Mol Sci* 24(22):16322
- Siddiqui WA, Ahad A, Ahsan H (2015) The mystery of BCL2 family: Bcl-2 proteins and apoptosis: an update. *Arch Toxicol* 89(3):289–317
- Sorinezami Z, Mansouri-Torshizi H, Aminzadeh M, Ghahghaei A, Jamgohari N, Heidari MM (2019) Synthesis of new ultrasonic-assisted palladium oxide nanoparticles: an in vitro evaluation on cytotoxicity and DNA/BSA binding properties. *J Biomol Struct Dyn* 37(16):4238–4250
- Tsikis D (2017) Assessment of lipid peroxidation by measuring malondialdehyde (MDA) and relatives in biological samples: analytical and biological challenges. *Anal Biochem* 524:13–30
- Urbani A, Prosdociami E, Carrer A, Checchetto V, Szabò I (2020) Mitochondrial ion channels of the inner membrane and their regulation in cell death signaling. *Front Cell Dev Biol* 8:620081
- Varunkumar K, Anusha C, Saranya T, Ramalingam V, Raja S, Ravikumar V (2020) Avicennia marina engineered nanoparticles induce apoptosis in adenocarcinoma lung cancer cell line through p53 mediated signaling pathways. *Process Biochem* 94:349–358
- Wang H, Fan Q, Zhang L, Shi D, Wang H, Wang S, Bian B (2020) Folate-targeted PTEN/AKT/P53 signaling pathway promotes apoptosis in breast cancer cells. *Pteridines* 31(1):158–164
- Wu Y-P, Yang J, Gao H-Y, Shen Y, Jiang L, Zhou C et al (2018) Folate-conjugated halloysite nanotubes, an efficient drug carrier, deliver doxorubicin for targeted therapy of breast cancer. *ACS Applied Nano Materials* 1(2):595–608
- Xu F, Zhang L, Heidari Majd M, Shiri F, Karimi P, Guo X (2023) Increase delivery, cytotoxicity, stability and induction of apoptosis in cisplatin by establishing a new complex with methotrexate. *J Drug Deliv Sci Technol* 86:104683
- Yan M, Majd MH (2021) Evaluation of induced apoptosis by biosynthesized zinc oxide nanoparticles in MCF-7 breast cancer cells using Bak1 and Bclx expression. *Dokl Biochem Biophys* 500(1):360–367
- Zhang X, Heidari MM (2023) Synthesis of halloysite nanotubes decorated with green silver nanoparticles to investigate cytotoxicity, lipid peroxidation and induction of apoptosis in acute leukemia cells. *Sci Rep* 13(1):17182
- Zsigrai S, Kalmár A, Barták BK, Nagy ZB, Szigeti KA, Valcz G et al (2022) Folic acid treatment directly influences the genetic and epigenetic regulation along with the associated cellular maintenance processes of HT-29 and SW480 colorectal cancer cell lines. *Cancers* 14(7):1820

## Publisher's Note

Springer Nature remains neutral with regard to jurisdictional claims in published maps and institutional affiliations.